

Bioinspired Synthesis of a Soft-Nanofilament-Based Coating Consisting of Polysilsesquioxanes/Polyamine and Its Divergent Surface Control

Jian-Jun Yuan,[†] Nobuo Kimitsuka,[‡] and Ren-Hua Jin^{*§}

[†]Synthetic Chemistry Laboratory, Kawamura Institute of Chemical Research, 631 Sakado, Sakura, Chiba 285-0078, Japan

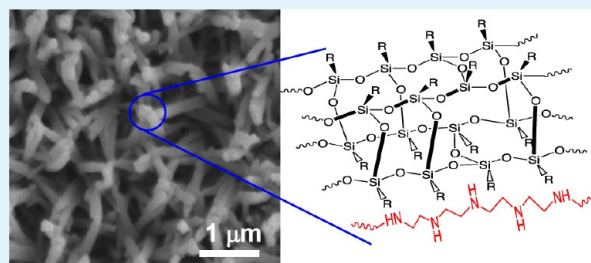
[‡]Department of Chemistry and Biochemistry, Graduate School of Engineering, Center for Molecular Systems (CMS), Kyushu University and JST-CREST, 744 Moto-oka, Nishi-ku, Fukuoka 819-0395, Japan

[§]Department of Material and Life Chemistry, Graduate School of Engineering, Kanagawa University and JST-CREST, 3-27-1, Rokkakubashi, Kanagawa-ku, Yokohama 221-8686, Japan

Supporting Information

ABSTRACT: The synthesis of polysilsesquioxanes coating with controllable one-dimensional nanostructure on substrates remains a major long-term challenge by conventional solution-phase method. The hydrolytic polycondensation of organosilanes in solution normally produces a mixture of incomplete cages, ladderlike, and network structures, resulting in the poor control of the formation of specific nanostructure. This paper describes a simple aqueous process to synthesize nanofilament-based coatings of polysilsesquioxanes possessing various organo-functional groups (for example, thiol, methyl, phenyl, vinyl, and epoxy). We utilized a self-assembled nanostructured polyamine layer as a biomimetically catalytic scaffold/template to direct the formation of one-dimensional nanofilament of polysilsesquioxanes by temporally and spatially controlled hydrolytic polycondensation of organosilane. The surface nanostructure and morphology of polysilsesquioxane coating could be modulated by changing hydrolysis and condensation reaction conditions, and the orientation of nanofilaments of polysilsesquioxanes on substrates could be controlled by simply adjusting the self-assembly conditions of polyamine layer. The nanostructure and polyamine@polysilsesquioxane hybrid composition of nanofilament-based coatings were examined by means of scanning electron microscopy (SEM), transmission electron microscopy (TEM), and X-ray photoelectron spectroscopy (XPS). The template role of nanostructured polyamine layer for the formation of polysilsesquioxane nanofilament was confirmed by combining thin film X-ray diffraction (XRD) and XPS measurements. Moreover, these nanotextured coatings with various organo-functional groups could be changed into superhydrophobic surfaces after surface modification with fluorocarbon molecule.

KEYWORDS: biomimetic synthesis, self-assembly, polysilsesquioxanes, nanofilament coating, superhydrophobic



INTRODUCTION

Coatings or thin films of polysilsesquioxanes (PSQ, formula of $\text{RSiO}_{1.5}$, where R is an organic group) are technologically important due to their excellent material properties and potential as precursors for functional ceramics.¹ PSQ film could be conventionally fabricated by coating silicone resins or forming self-assembled monolayer silanes on substrates.² However, these methods are inherently not in favor of forming coatings with controlled nanostructure and surface morphology, which is potentially important for applications in the superliquid-repelling and biomedical fields.^{3–8} Recently, a few reports described the synthesis of nanofilament coatings of PSQ on substrate surface via vapor-phase or solvent-phase reactions with careful control of relative humidity.^{3–7} However, these methods are normally limited to caustic trichloromethylsilane with complicated procedure and also have difficulties in control of the size, morphology, and orientation of the nanofilament on the substrates.

Recently, construction of materials systems by learning from nature has become a new emerging field.^{9–12} One of the merits of nature-inspired materials synthesis is to harness the mild yet efficient chemical process developed in biological systems for creating artificial functional materials. It is widely known that diatoms and sponges grow their siliceous skeletons via biosilicification with precisely controlled nanopattern, hierarchical morphology, and organic–inorganic hybrid structure under ambient conditions.^{13,14} This natural process has inspired the synthesis of nanostructured silica by designing organic matrices which work as catalyst and templates.¹⁵ However, the biosilicification has rarely been applied to biomimetic synthesis of PSQ through organosilane deposition. It is known that the sol–gel reaction of organosilanes in solution normally produces

Received: January 3, 2013

Accepted: March 27, 2013

Published: March 27, 2013

the mixture of incomplete cages, ladderlike structures, and network structures.¹⁶ This makes it difficult to control nanostructure and maintain the structure stability on a substrate surface after drying. Therefore, it is very challenging to construct the PSQ coatings with controlled nanostructure and surface morphology on a substrate surface. In 1999, Cha et al.¹⁷ reported that silicatein filaments isolated from a marine sponge could direct the biomimetic silica formation. In their paper, the authors mentioned that the silicatein filaments could also accelerate hydrolysis and condensation of phenyltrimethoxysilane (PTMS) and methyltrimethoxysilane (MTMS). To the best of our knowledge, the biomimetic synthesis of polysilsesquioxanes with controlled nanostructure directed by a designed organic-template system has not yet been reported. Therefore, it is both scientifically interesting and technologically significant to establish a new concept for constructing nanostructured polysilsesquioxanes by mimicking the silica mineralization in organisms.

Herein, we report a biosilicification-inspired approach to generate polysilsesquioxanes (PSQ) nanofilament coatings by using a self-assembled polyamine as a template that assists spatially controlled hydrolytic polycondensation of organotrimethoxysilanes under ambient conditions. Unlike previous vapor- or solvent-phase studies that are very limited to synthesis of methyl- or vinyl-polysilsesquioxanes,^{3–7} our biomimetic approach could generally offer polysilsesquioxane nanofilament coatings with various organic functional groups, including thiol, olefine, and epoxy that are important for subsequent chemical modification or biological functionalization.¹⁸ Moreover, simple adjustment of the conditions for polyamine self-assembly or sol-gel reaction of organosilanes could lead to the precise control on nanostructure and orientation of nanofilaments on substrate surface, which still remains major challenge for previous vapor- or solvent-phase methods.^{3–7} Moreover, nanostructure control and surface modification afforded a superliquid-repellent function on the coatings with various organo-functions.

■ EXPERIMENTAL SECTION

Materials. Linear polyethylenimine (LPEI) was synthesized by hydrolysis of poly(2-ethyl-2-oxazoline)s.¹⁹ The organosilanes of 3-mercaptopropyltrimethoxysilane (MPS), methyltrimethoxysilane (MTMS), vinyltrimethoxysilane (VTMS), 3-glycidoxypropyltrimethoxysilane (GPMS), and phenyltrimethoxysilane (PTMS) were provided by Shinetsu Co. Japan. HD 1101Z (perfluoro polyether with a silane coupling end group) was purchased from Daikin Co. Japan, respectively.

Formation of PSQ Nanofilaments on Substrates. The LPEI layer was prepared by dipping substrates into 3 wt % hot aqueous solution (80 °C) of LPEI, and then keeping the hot substrates covered with aqueous LPEI in air at 20 °C for 20–30 s for the formation of nanostructured LPEI layers.²⁰ The PSQ deposition was performed by immersing the nanostructured LPEI@substrates into an aqueous source of organosilanes at room temperature for 4–120 h under nearly neutral conditions. The source was prepared by simply adding organosilanes into 50 mL of water with the concentrations of organosilanes ranging from 0.1 to 4.0 vol %. The mixture of organosilanes and water was directly used for hydrolysis and condensation reaction, and no any additive acid or base was used for prehydrolyzation of organosilanes. Typically, the organosilanes are not miscible in water, the dispersed droplets of organosilanes in water serves as a reservoir for the hydrolysis and polycondensation.

The fluorocarbon modification of PSQ coatings was carried out by immersing the coatings into HD-1101Z (perfluoro polyether with a

silane coupling end group, Daikin Co. Japan) for 24 h and then drying at ambient conditions.

Characterizations. The surface morphology of PSQ coatings was observed using scanning electron microscopy instrument (SEM, Keyence, VE9800, Japan). Transmission electron microscopy (TEM) studies were conducted on a JEOL JEM-2200FS instrument operating at 200 kV. Thin film X-ray diffraction measurements (XRD) were carried out with a Rigaku RINT-TTR II diffractometer (Rigaku co., Japan), using Cu K α radiation ($\lambda = 1.54 \text{ \AA}$). X-ray photoelectron spectroscopy (XPS) measurements were carried out on a PHI Quantera SXM spectrometer. The degree of polycondensation (T3, T2, and T1) of PSQ was characterized by ²⁹Si CP MAS NMR spectroscopy, and the spectra were recorded on a JEOL-400 MHz NMR spectrometer. The contact angle (CA) of coatings was measured using an optical contact angle meter (OCA20, DataPhysics, Germany) with a liquid drop of 5 μ L.

■ RESULTS AND DISCUSSION

For biomimetic fabrication of soft-nanofilament coatings of polysilsesquioxanes, an organized polyamine layer formed by crystallization-driven self-assembly of linear polyethylenimine (LPEI, possessing only secondary amine units [NHCH₂CH₂]_n in its backbone) on substrates was used as catalytic scaffold/template for hydrolytic polycondensation of organosilanes. We integrated our earlier work of synthesis of LPEI-mediated silica/titania nanograss²⁰ to the present synthesis of polysilsesquioxanes coatings. First, self-assembled crystalline LPEI layer on substrates was prepared via a simple pathway, which involves dipping the substrates into a hot aqueous solution of LPEI for polymer adsorption and then keeping the hot substrates in air or in water at room temperature. Secondly, the polysilsesquioxanes coatings were synthesized by immersing the substrates covered with self-assembled LPEI layer into a mixture of water and organosilanes at room temperature (for details, see the Supporting Information).

Since the thiol (–SH) group has significant potential for materials science and nanotechnology,²¹ we first attempted to deposit poly(mercaptopropylsilsesquioxane) (pSi–SH) nanofilament coating using 3-mercaptopropyltrimethoxysilane (MPS) as a source. This hydrolytic polycondensation of MPS was performed by immersing the substrates with self-assembled LPEI layer into a mixture of 50 mL water and 0.25 mL MPS for 15 h at room temperature. Interestingly, no pSi–SH particles generated owing to sol-gel reaction were observed in the aqueous phase, indicating that this reaction of MPS selectively occurs via hydrolytic polycondensation on the self-assembled LPEI layer on the substrate. SEM observation indicated the formation of the uniform coating on glass substrate with well-defined grass-like structure (Figure 1a). The high-magnification SEM image showed that the coating is composed of densely arrayed nanofilaments of about 200 nm in width (Figure 1b) and the coating thickness is typically about 2.5 μ m (Figure 1c). TEM examination of the filaments scraped from the coating film supported that the filament has ribbonlike structure (Figure 1d). It is extremely different to the conventional polysilsesquioxane coatings prepared via vapor- or solvent-phase separation process which only produce network structure of nanofilament rather than such vertical orientation of nanofilaments on substrate.^{3–6} In our case, the unique crystallization-driven self-assembly of LPEI¹⁹ affords the formation of a vertically arrayed LPEI nanofilaments layer on the substrate by naturally cooling the hot LPEI-adsorbed substrate.²⁰ The self-assembled LPEI nanofilaments serve as templates to direct the formation of vertically arrayed pSi–SH-

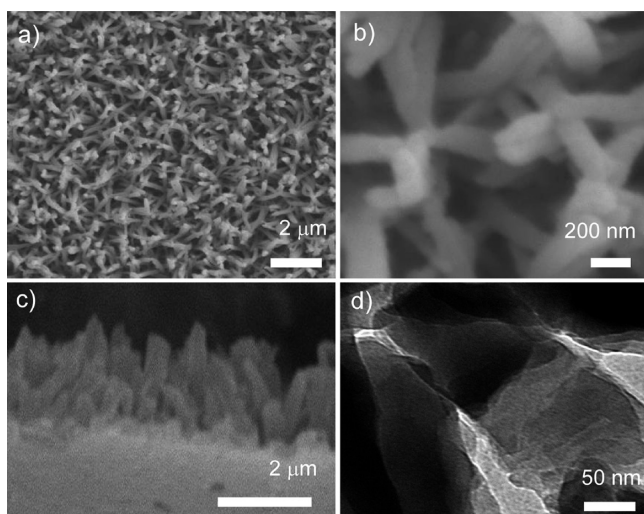


Figure 1. SEM (a–c) and TEM (d) images of LPEI@pSi-SH nanofilament coating on a glass substrate. Self-assembled LPEI layers were formed by first dipping substrates into hot LPEI aqueous solution (3.0 wt %) for polymer adsorption and then keeping hot substrates@LPEI in air at 20 °C for 20–30 s. The MPS deposition was performed by dipping glass substrate covered with self-assembled LPEI layer into a mixture of 50 mL of water and 0.25 mL of MPS at room temperature for 15 h.

based nanofilament coating. The hydrolytic polycondensation of MPS occurs in a temporally and spatially controlled manner on the LPEI template, leading to the formation of LPEI@pSi-SH hybrid nanofilaments.

To examine the template role of LPEI for organosilane deposition, we carried out the measurements of XPS and thin film XRD. Figure 2a shows XRD profiles of self-assembled LPEI layer on substrate and LPEI@pSi-SH nanofilament

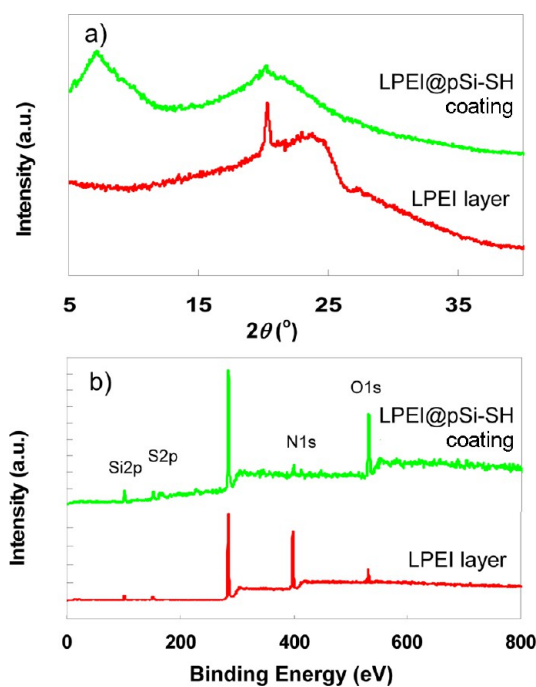


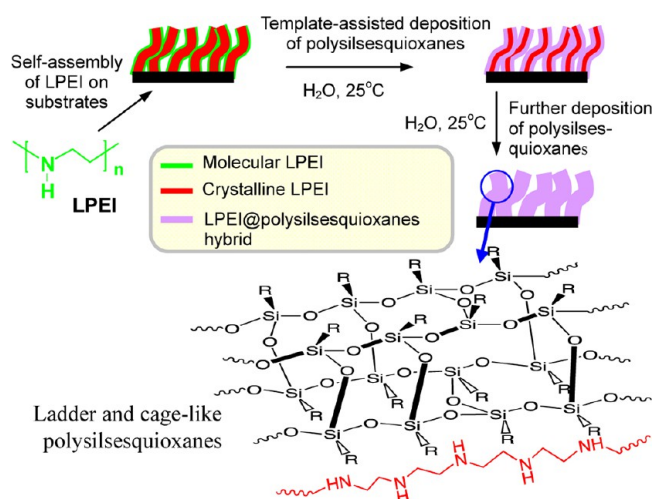
Figure 2. XRD (a) and XPS (b) profiles for self-assembled LPEI layer on substrate and LPEI@pSi-SH nanofilament coating. The synthetic conditions are the same as those used in Figure 1.

coating. Before the hydrolytic polycondensation, the LPEI layer sharply scattered at $2\theta = 20.0^\circ$ due to the crystalline LPEI (Figure 2a). After hydrolytic polycondensation, however, this peak nearly disappears due to the formation of LPEI@pSi-SH coating (Figure 2a). This is very different to the case of silica deposition, where crystalline LPEI template still exists after the formation of silica nanofilaments.²⁰ In addition to the disappearance of crystalline LPEI peak, a new peak appeared at $2\theta = 7.8^\circ$ (corresponding $d = 1.13$ nm) for the LPEI@pSi-SH coating, which could be attributed to the presence of interval spacing structures with long-range orders in the nanofilament of the polysilsesquioxane.²² For LPEI layer on substrate, XPS profile shows the peak at 400 eV (N1s) due to N atom in LPEI (Figure 2b). After hydrolytic polycondensation of MPS, the characteristic signals due to silicon (Si2p at 103 eV) and sulfur (S2p at 153 eV) were detected (Figure 2b), confirming the successful polymerization of MPS. In addition, a weak nitrogen peak (N1s at 400 eV) is still detected for the nanofilament coating, indicative of the hybrid feature of LPEI@pSi-SH.

To further understand the catalytic template role of LPEI nanofilament for hydrolytic polycondensation of MPS, the LPEI aggregates dispersed in water were used for the reaction of MPS under the conditions comparative to that used for nanofilament coating shown in Figure 1. Both SEM and TEM observation confirmed the nanofilament formation of LPEI@pSi-SH (Supporting Information Figure S1a–d). Solid-state ²⁹Si CP/MAS NMR measurement (see Figure S1e) indicated the integration values of the different bonding 91.2 (T3), 8.8 (T2), and zero (T1) from which T3/(T2 + T3 + T1) is calculated as 91.8. This reveals that the LPEI templates effectively promote the hydrolytic polycondensations of MPS. Considering the interval structure appearance as seen in XRD, the high degree of T3 bonding strongly supports that the poly(mercaptopropylsilsesquioxane) possesses ladder and/or cage-like structures in its backbone.

Accordingly, we propose a mechanism for the formation of the LPEI@pSi-SH hybrid nanofilament coating (Scheme 1). The self-organized LPEI crystalline filaments on substrate

Scheme 1. Schematic Representation for Plausible Mechanism of the Formation of Nanofilament Coating of LPEI@polysilsesquioxanes Assisted by Self-Assembled LPEI Layer on Substrate as a Temporary Sacrificial Template for Spatially Controlled Sol–Gel Reaction of Organosilanes



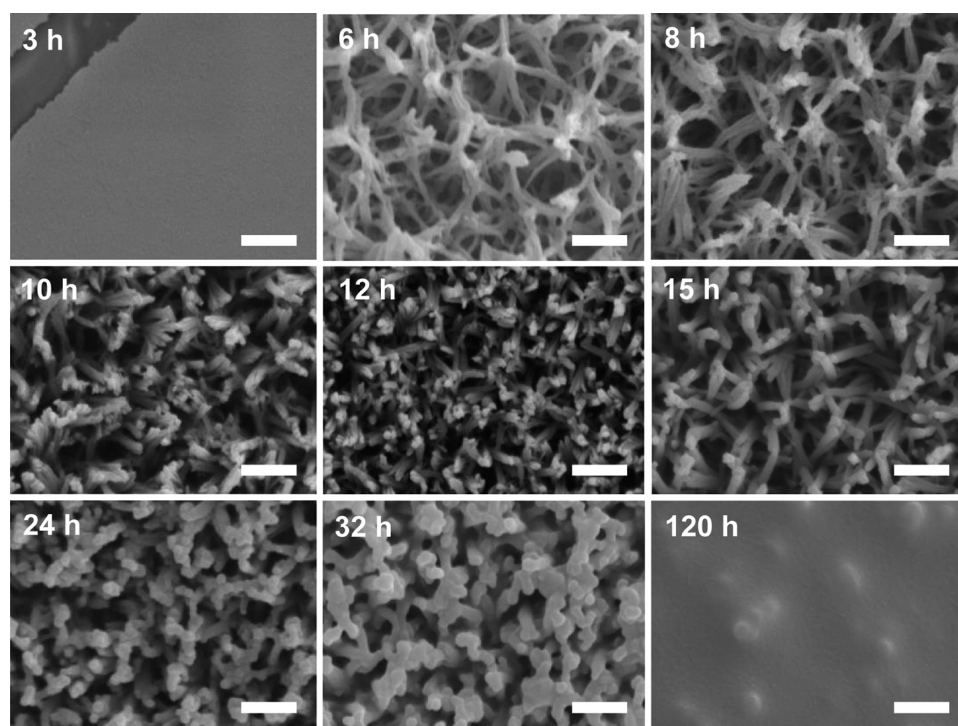


Figure 3. SEM images of LPEI@pSi-SH coatings prepared with various reaction times. Self-assembled LPEI layers were formed by first dipping the substrates into hot LPEI aqueous solution (3.0 wt %) for polymer adsorption and then keeping hot substrates@LPEI in air at 20 °C for 20–30 s. The MPS deposition was performed by dipping glass substrate covered with self-assembled LPEI layer into a mixture of 50 mL of water and 0.25 mL of MPS at room temperature. The scale bars are 1 μm for each case.

promote site-selective hydrolytic polycondensation of MPS around the LPEI filaments on which the ladder/cagelike backbones of pSi-SH grows. With the growth of pSi-SH, the crystallinity of the LPEI template gradually disordered and finally hybridized into the resulting polysilsesquioxane network, leading to the simultaneous formation of LPEI@pSi-SH hybrid nanofilament structure. We assume that the intervals between the ladderlike structure of poly-(mercaptopropylsilsesquioxane)s provides molecular-scale space for the hybridization of the disordered LPEI. As far as we are aware, this is a first example of the synthesis of one-dimensional nanostructure by using MPS as single organosilane source. On the basis of the conventional Stöber method, a few reports described the synthesis of thiol-based spherical particles in solution by base-catalyzed hydrolysis and polycondensation of MPS.¹⁸

Our bioinspired approach further allows the rational design of nanostructure and surface morphology of LPEI@pSi-SH nanofilament coating by simply regulating the conditions including hydrolytic polycondensation time, organosilane concentrations, or LPEI self-assembly. We found that a thin flat film without textured structure was produced when the LPEI-layer substrate was dipped into MPS solution for 3 h (Figure 3 and Supporting Information Figure S2). This would be due to the fact that the short reaction time could not give a mature polysilsesquioxane that can support the textured structures. The extended reaction times (i.e., dipping times) from 6–12 h led to the well-defined nanofilament coatings, and the size and density of nanofilaments gradually increase with the increase of deposition times (Figure 3 and Figure S2). When the reaction time reached to 15 h, the coating showed the decrease of nanofilament density with a slight increase of the diameter of elemental nanofilaments. When the reaction time

was further increased to 120 h, a thick coating (10 μm) without nanofilament structure was produced (Figure 3 and Figure S2). Such systematic control of nanostructure of LPEI@pSi-SH coating could be also achieved by changing MPS concentrations from 0.1 to 2.0 vol % by fixing reaction time of 15 h (Supporting Information Figures S3 and S4). It seems that there is an appropriate range of quantity of polysilsesquioxane for support the nanofilament coating. Either too small or too large a quantity of polysilsesquioxane does not yield the nanofilament coatings.

We have previously demonstrated that crystallization-driven self-assembly of LPEI could be modulated with physical or chemical quenching by performing the LPEI crystallization in neutral or alkali water, leading to the controlled formation of silica nanowire or nanotube structure with 10 nm diameter.^{23,24} Here, LPEI layers prepared by the modified self-assembly conditions (such as quenching in neutral or alkali water)^{23,24} were employed in the same hydrolytic polycondensation of MPS for comparison of the formation of polysilsesquioxane coatings. As shown in Figure 4a and b, interestingly, a coating composed of nanowire-based network structure of pSi-SH was formed by using an LPEI layer that was prepared by dipping hot LPEI@substrate into water bath at 20 °C for rapid crystallization (physical quenching). In this system, the surface patterns of the LPEI@pSi-SH nanowire-based coatings could be also tunable by changing dipping reaction time from 4 to 24 h (Supporting Information Figure S5).

Furthermore, we found that surface component of LPEI@pSi-SH nanowire-based coatings is dependent on the reaction time. On the basis of the time-course profiles of XPS, it was confirmed that the intensity of the peak due to N1s from LPEI gradually decrease when the reaction time increases (Figure 5). This suggested that the surface quantity of the pSi-SH

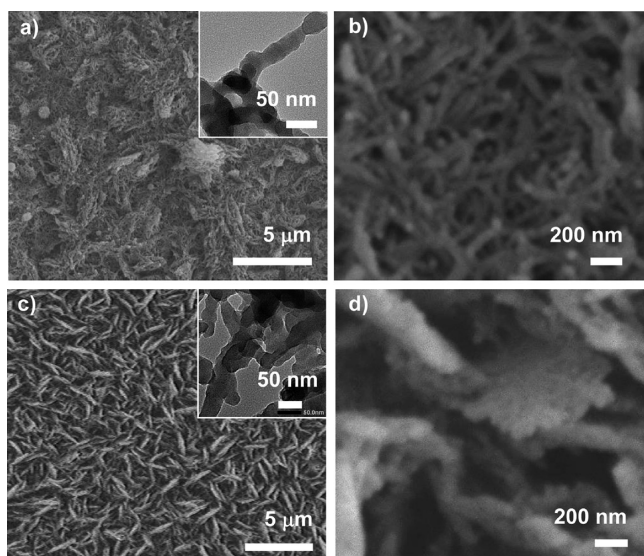


Figure 4. Nanowire-based LPEI@pSi-SH coatings prepared by using LPEI layers which were formed by dipping hot substrate@LPEI into a water bath for rapid crystallization of LPEI (a and b) and dipping substrate covered with protonated LPEI into 0.5 M NaOH solution for alkali-induced LPEI self-assembly (c and d). The MPS deposition conditions are the same as that used in Figure 1. The insets of a and c are TEM images for showing the elemental nanowire structure.

hybridized with the LPEI filaments increased with the increase of the dipping time.

We also found that a hierarchically structured coating with LPEI@pSi-SH nanowire as an elemental nanostructure could be easily produced when LPEI self-assembly was performed by an alkali-induced process (chemical quenching). As shown in Figure 4c and d and Supporting Information Figure S6, the coating is composed of high-density two-dimensional mat of ca. 1–2 μm in diameter. The mats grew vertically from the substrate with random orientation. The TEM and high-magnification SEM images demonstrated that the mat is very thin and composed of nanowire structure of about 50–100 nm in diameter.

Different from the previous report of nanofilament coatings from vapor- or solvent-phase by using methyl or vinyl

trichlorosilanes that are normally limited to the formation of nanowire-based network structure,^{3–7} our LPEI-assisted biomimetic approach could offer the rational design of filament nanostructure/orientation and surface morphology of polysilsesquioxane coatings by simply modulating LPEI self-assembly or hydrolytic polycondensation conditions of organosilanes.

Since the surface of the coating of LPEI@pSi-SH is abundant in thiol groups, this coating is potentially widely applicable in chemical modifications. We preliminarily performed a thiol-ene click reaction^{25–27} by immersion of nanofilament-based LPEI@pSi-SH coating into 2-ethylpentyl acrylate (EPA) at room temperature for 2 h in the presence of dimethylphenylphosphine (as catalyst).²⁸ SEM observation indicated that the click reaction did not give rise to any change of surface nanostructure of LPEI@pSi-SH (Supporting Information Figure S7). Surface wettability studies suggested that, after click reaction, the water contact angles increased from 97.1° to 133.3°, indicating the efficient introduction of EPA residues onto the coating (see Figure S7).

To demonstrate the general feature of this coating approach, we extend this method toward a series of organosilanes with various organic groups, including methyltrimethoxysilane (MTMS = CH₃), vinyltrimethoxysilane (VTMS = V), 3-glycidoxypropyltrimethoxysilane (GPTMS = EP), phenyltrimethoxysilane (PTMS = Ph), and a mixture of MPS and VTMS (SH and V, molar ratio 1–1). As shown in Figure 6, the well-defined nanofilament coatings of LPEI@pSi-CH₃, LPEI@pSi-V, LPEI@pSi-EP, LPEI@pSi-Ph, and LPEI@pSi-SH/V were successfully achieved under suitable reaction conditions (time and/or organosilane concentration).

Moreover, all coatings exhibited excellent tunability of filament nanostructure by changing the reaction conditions (see SEM images in Supporting Information Figures S8–S12). By means of XPS measurements, we examined the surface composition of these nanofilament coatings. As shown in Figure 7, characteristic signals due to silicon (Si2p at 103 eV and Si2s at 155 eV) were detected for the curves from all coatings, confirming the successful deposition of organosilanes. High-resolution XPS curves demonstrated that the peak at 400 eV (N1s) due to N atom in LPEI appears for coatings of LPEI@pSi-CH₃, LPEI@pSi-V, LPEI@pSi-EP, and LPEI@pSi-

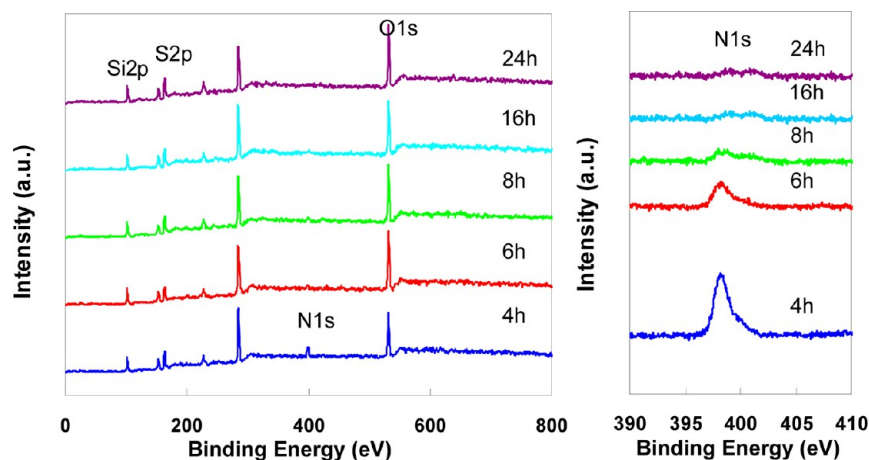


Figure 5. XPS curves of nanowire-based LPEI@pSi-SH coatings prepared with the MPS deposition times of 4, 6, 8, 16, and 24 h. Self-assembled LPEI layers were formed by dipping hot substrate@LPEI into water bath for rapid crystallization of LPEI.²⁵ The MPS deposition conditions are the same as that used in Figure 1.

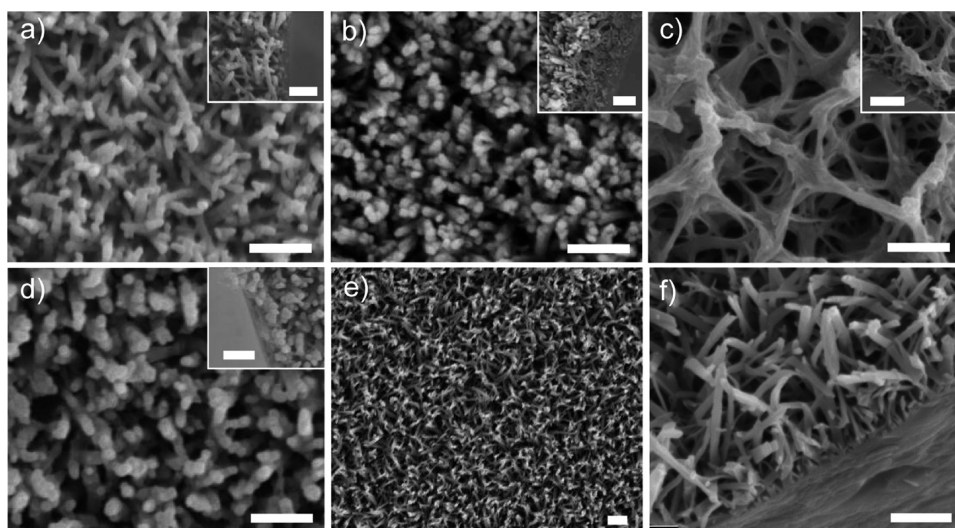


Figure 6. SEM images of nanofilament coatings of LPEI@pSi-CH₃ (a), LPEI@pSi-V (b), LPEI@pSi-EP (c), LPEI@pSi-Ph (d), and LPEI@pSi-SH/V (e and f). The insets of a–d are the cross-section SEM images of a–d, respectively. (f) Cross-section SEM images of part e. Self-assembled LPEI layers were formed by first dipping substrates into hot LPEI aqueous solution (3.0 wt %) for polymer adsorption and then keeping hot substrates@LPEI in air at 20 °C for 20–30 s. The depositions of various organosilanes were performed by dipping the substrate covered with self-assembled LPEI layer into a mixture of 50 mL water and organosilanes at room temperature. The nanofilament coatings of LPEI@pSi-CH₃, LPEI@pSi-V, LPEI@pSi-EP, LPEI@pSi-Ph, and LPEI@pSi-SH/V were prepared by using 0.5 mL of MTMS with reaction time of 48 h, 0.25 mL of VTMS with reaction time of 15 h, 0.5 mL of GPTMS with reaction time of 18 h, 0.3 mL of PTMS with reaction time of 7 h, and 0.3 mL of MPS/VTMS (1–1 molar ratio) with reaction time of 15 h, respectively. The bars are 1 μm for each case.

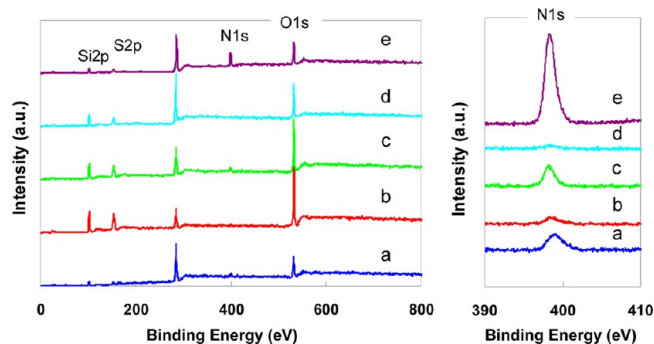


Figure 7. XPS curves of nanowire-based coatings of LPEI@pSi-SH (a), LPEI@pSi-CH₃ (b), LPEI@pSi-V (c), LPEI@pSi-Ph (d), and LPEI@pSi-EP (e). The synthetic conditions are identical to that used for Figure 6. The left is the high-resolution curves for N1s.

SH/V, indicating the presence of LPEI segments on the surface or shallow region of nanofilament. As an exception, no N1s signal was observed for LPEI@pSi-Ph, suggesting that LPEI probably has been encapsulated in the deep inner region of LPEI@pSi-Ph filaments.

In general, polysilsesquioxanes are chemically and physically robust compared with organic polymers and could improve mechanical stability.³ Such advantages should benefit for applications of nanofilament-based polysilsesquioxanes coatings in superhydrophobic materials. As shown in Figure 8a, the native pSi-SH coating with vertically arrayed nanofilament nanostructure (Figure 1) demonstrated a water contact angle (CA) of 97°. After surface modification with perfluoro polyether (HD 1101Z), the coatings (f-pSi-SH) become superhydrophobic with a water contact angle of 177.7°. To demonstrate the possibility of our superhydrophobic surface for practical technological application,²⁴ we further evaluated the wettability of f-pSi-SH coatings toward a mixture liquid of water–ethanol (1:1 in vol). We found that f-pSi-SH coating

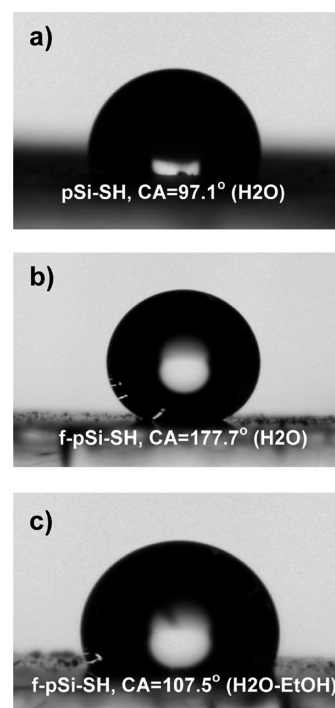


Figure 8. Contact angles of water (a and b) and water–ethanol mixture with a composition of 1:1 in volume (c) on the nanofilament-based surfaces of native pSi-SH (a) and f-pSi-SH (b and c, after fluorocarbon modification).

shows a contact angle of 107.5° toward water–ethanol mixture (Figure 8c).

The contact angles of nanofilament coatings possessing various organic groups were compared, and the results were summarized in Figure 9 and Supporting Information Figure S13. The original nanofilament coatings with different organic

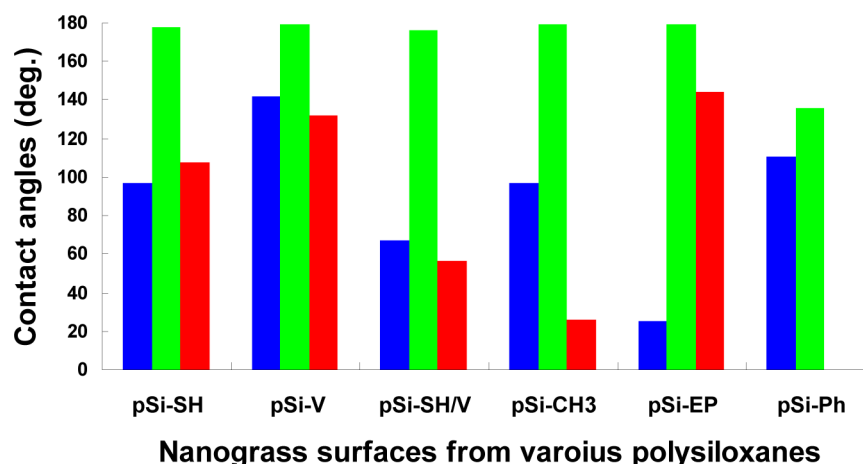


Figure 9. Surface wettability of the nanofilament coatings from various polysilsesquioxanes: (blue) water CAs of native coatings; (green) water CAs of coatings after fluorocarbon treatment; (red) CAs of fluorocarbon-treated coatings for a liquid of ethanol–water mixture with a 1–1 volume ratio. The synthetic conditions of nanofilament coatings are the same as those used in Figure 1 for pSi–SH and Figure 6 for pSi–V, pSi–SH/V, pSi–CH₃, pSi–EP, and pSi–Ph.

silane residues of pSi–SH, pSi–V, pSi–SH/V, pSi–CH₃, pSi–EP, and pSi–Ph (see Figures 1 and 6 for SEM images) showed the water contact angles of 97.0°, 141.5°, 67.0°, 97.2°, 25.1°, and 110.7°, respectively. The pSi–V coatings with vinyl-terminated surface showed the relatively high water contact angles in contrast to those of pSi–CH₃ (methyl-terminated) and pSi–Ph (phenyl-terminated). This could be partially attributed to the difference of surface nanostructure. Compared to the coatings of pSi–CH₃ and pSi–Ph, the pSi–V coating exhibited significantly denser and smaller nanofilaments structure.

After fluorocarbon modification, the coatings of f-pSi–SH, f-pSi–V, f-pSi–SH/V, f-pSi–CH₃, and f-pSi–EP became super-hydrophobic with water contact angles higher than 176°, indicative of nearly perfect nonwetting (Figure 9 and Supporting Information Figure S13). The fluorocarbon-treated coating of phenyl-terminated surface (f-pSi–Ph) showed a water contact angle of 135.8°, due to low surface roughness (Figure 9 and Figure S13). For the coatings of f-pSi–V, f-pSi–CH₃, and f-pSi–EP, we could not determine the water contact angles because water droplet cannot stably rest on their surface (Figure S13).

We further evaluated the wettability of our fluorocarbon-treated coatings toward a mixed liquid of ethanol–water (1–1 in vol). It was found that f-pSi–SH, f-pSi–V, f-pSi–SH/V, f-pSi–CH₃, and f-pSi–EP coatings exhibited the contact angles of 107.5°, 131.6°, 56.2°, 26.3° and 143.9°, respectively (Figure 9 and Supporting Information Figure S13). We have previously demonstrated that fluorocarbon-modified nanostructured silica surfaces could be perfectly nonwetting toward the mixed liquid of ethanol–water (1–1 in vol) and even a commercial IJ ink (blue, Canon Japan).^{24,29} In contrast, the current polysilsesquioxanes coatings showed the significantly decreased contact angles toward ethanol–water mixed liquid because these polysilsesquioxanes surfaces generally have a decreased surface roughness compared to the nanostructured silica surfaces.^{24,29} In addition, the contact angles toward ethanol–water mixed liquid is dramatically different for the coatings from f-pSi–SH, f-pSi–V, f-pSi–SH/V, f-pSi–CH₃, and f-pSi–EP coatings. This could be partially due to the difference of surface roughness, surface chemistry, and efficiency of fluorocarbon modification. However, the exact reason for this wettability difference due to

the different polysilsesquioxanes is currently not clear; related studies are still under progress.

CONCLUSIONS

In summary, we have successfully demonstrated a biomimetic aqueous approach to the synthesis of soft-nanofilament coatings of hybrid polysilsesquioxanes/polyamine by using a self-assembled LPEI layer as a catalytic template for hydrolytic polycondensation of organosilanes. This approach allows the precise control of the nanostructure and orientation of the nanofilament of polysilsesquioxanes by simply modulating either crystallization-driven self-assembly of LPEI layers or hydrolytic polycondensation conditions of organosilanes. Especially, the soft-nanofilaments of poly-(mercaptopropylsilsesquioxane) coating could be potentially applicable in a wide range of technological fields by exploiting versatile thiol chemistry such as click reaction^{25–28} and bioengineering.³⁰ The nanotextured coatings are structurally stable toward a series of solvents (Supporting Information Figure S14) and showed the tunable surface wettability. Moreover, this aqueous, room-temperature process has been further extended to general synthesis of nanofilament coatings of polysilsesquioxanes with various organo-functions.

ASSOCIATED CONTENT

Supporting Information

Figures showing SEM and TEM images and ²⁹Si CP-MAS NMR profile of LPEI@pSi–SH powder prepared in solution, SEM images of polysilsesquioxane coatings synthesized under various conditions, and contact angles of various coatings. This material is available free of charge via the Internet at <http://pubs.acs.org/>.

AUTHOR INFORMATION

Corresponding Author

*Tel.: +81-45-481-5661 (ext 3845). E-mail: rhjin@kanagawa-u.ac.jp.

Notes

The authors declare no competing financial interest.

ACKNOWLEDGMENTS

This research was partly supported by Core Research for Evolutional Science and Technology (CREST), Japan Science and Technology Corporation (JST).

REFERENCES

- (1) Baney, R. H.; Itoh, M.; Sakakibara, A.; Suzuki, T. *Chem. Rev.* **1995**, *95*, 1409–1430.
- (2) Plueddemann, I. P. *Silane Coupling Agents*; Plenum: New York, 1991.
- (3) Artus, G. R. J.; Jung, S.; Zimmermann, J.; Gautschi, H.-P.; Marquardt, K.; Seeger, S. *Adv. Mater.* **2006**, *18*, 2758–2762.
- (4) Gao, L.; McCarthy, T. J. *J. Am. Chem. Soc.* **2006**, *128*, 9052–9053.
- (5) Rolling, D. E.; Veinot, J. G. C. *Langmuir* **2008**, *24*, 13653–13662.
- (6) Jin, M.; Wang, J.; Yao, X.; Liao, M.; Zhao, Y.; Jiang, L. *Adv. Mater.* **2011**, *23*, 2861–2864.
- (7) Ke, Q.; Li, G.; Liu, Y.; He, T.; Li, X.-M. *Langmuir* **2009**, *26*, 3579–3584.
- (8) Zimmermann, J.; Rabe, M.; Verdes, D.; Seeger, S. *Langmuir* **2008**, *24*, 1053–1057.
- (9) Nudelman, F.; Sommerdijk, N. A. J. M. *Angew. Chem., Int. Ed.* **2012**, *51*, 6582–6596.
- (10) Kröger, N.; Poulsen, N. *Ann. Rev. Gene* **2008**, *42*, 83–107.
- (11) Xia, F.; Jiang, L. *Adv. Mater.* **2008**, *20*, 2842–2858.
- (12) Meldrum, F. C.; Cölfen, H. *Chem. Rev.* **2008**, *108*, 4332–4432.
- (13) Schröder, H. C.; Wang, X.; Tremel, W.; Ushijima, H.; Müller, W. E. G. *Nat. Prod. Rep.* **2008**, *25*, 455–474.
- (14) Brutchey, R. L.; Morse, D. E. *Chem. Rev.* **2008**, *108*, 4915–4934.
- (15) Patwardhan, S. V.; Clarson, S. J.; Perry, C. C. *Chem. Commun.* **2005**, 1113–1121.
- (16) Loy, D. A.; Baugher, B. M.; Baugher, C. R.; Schneider, D. A.; Rahimian, K. *Chem. Mater.* **2000**, *12*, 3624–3632.
- (17) Cha, J. N.; Shimizu, K.; Zhou, Y.; Christiansen, S. C.; Chmelka, B. F.; Stucky, G. D.; Morse, D. E. *Proc. Natl. Acad. Sci. U.S.A.* **1999**, *96*, 361–365.
- (18) Nakamura, M.; Ishimura, K. *Langmuir* **2008**, *24*, 12228–12234.
- (19) Yuan, J.-J.; Jin, R.-H. *Langmuir* **2005**, *21*, 3136–3145.
- (20) Jin, R.-H.; Yuan, J.-J. *Adv. Mater.* **2009**, *21*, 3750–3753.
- (21) Hoyle, C. E.; Lowe, A. B.; Bowman, C. N. *Chem. Soc. Rev.* **2010**, *39*, 1355–1387.
- (22) Dong, F.; Guo, W.; Park, S.-S.; Ha, C.-S. *J. Mater. Chem.* **2011**, *21*, 10744–10749.
- (23) Yuan, J.-J.; Jin, R.-H. *J. Mater. Chem.* **2012**, *22*, 5080–5088.
- (24) Yuan, J.-J.; Jin, R.-H. *Langmuir* **2011**, *27*, 9588–9596.
- (25) Hoyle, C. E.; Bowman, C. N. *Angew. Chem., Int. Ed.* **2010**, *49*, 1540–1573.
- (26) Hensarling, R. M.; Hoff, E. A.; LeBlanc, A. P.; Guo, W.; Rahane, S. B.; Patton, D. L. *J. Polym. Sci. Part A: Polym. Chem.* **2013**, *51*, 1079–1090.
- (27) Sparks, B. J.; Ray, J. G.; Savin, D. A.; Stafford, C. M.; Patton, D. L. *Chem. Commun.* **2011**, *47*, 6245–6247.
- (28) Chan, J. W.; Hoyle, C. E.; Lowe, A. B. *J. Am. Chem. Soc.* **2009**, *131*, 5751–5753.
- (29) Yuan, J.-J.; Jin, R.-H. *J. Mater. Chem.* **2011**, *21*, 10720–10729.
- (30) Yang, S.; Ko, E.; Jung, Y.; Choi, I. *Angew. Chem., Int. Ed.* **2011**, *50*, 6115–6118.